

UC Davis

UC Davis Previously Published Works

Title

High-resolution Fourier-Domain Optical Coherence Tomography and Microperimetric Findings After Macula-off Retinal Detachment Repair

Permalink

<https://escholarship.org/uc/item/93x5030v>

Journal

Ophthalmology, 115(11)

ISSN

0161-6420

Authors

Smith, Allison J
Telander, David G
Zawadzki, Robert J
et al.

Publication Date

2008-11-01

DOI

10.1016/j.opthta.2008.05.025

Peer reviewed

High-resolution Fourier-Domain Optical Coherence Tomography and Microperimetric Findings After Macula-off Retinal Detachment Repair

Allison J. Smith, MD, David G. Telander, MD, PhD, Robert J. Zawadzki, PhD, Stacey S. Choi, PhD, Lawrence S. Morse, MD, PhD, John S. Werner, PhD, Susanna S. Park, MD, PhD

Objective: To evaluate the morphologic changes in the macula of subjects with repaired macula-off retinal detachment (RD) using high-resolution Fourier-domain optical coherence tomography (FD OCT) and to perform functional correlation in a subset of patients using microperimetry (MP-1).

Design: Prospective observational case series.

Participants: Seventeen eyes from 17 subjects who had undergone anatomically successful repair for macula-off, rhegmatogenous RD at least 3 months earlier and without visually significant maculopathy on funduscopy.

Methods: FD OCT with axial and transverse resolution of 4.5 μm and 10 to 15 μm , respectively, was used to obtain rapid serial B-scans of the macula, which were compared with that from Stratus OCT. The FD OCT B-scans were used to create a 3-dimensional volume, from which *en face* C-scans were created. Among 11 patients, MP-1 was performed to correlate morphologic changes with visual function.

Main Outcome Measures: Stratus OCT scans, FD OCT scans, and MP-1 data.

Results: Stratus OCT and FD OCT images of the macula were obtained 3 to 30 months (mean 7 months) postoperatively in all eyes. Although Stratus OCT revealed photoreceptor disruption in 2 eyes (12%), FD OCT showed photoreceptor disruption in 13 eyes (76%). This difference was statistically significant ($P < 0.001$, χ^2). Both imaging modalities revealed persistent subretinal fluid in 2 eyes (12%) and lamellar hole in 1 eye. Among 7 subjects who had reliable MP-1 data, areas of abnormal function corresponded to areas of photoreceptor layer disruptions or persistent subretinal fluid in 5 subjects (71%); one subject had normal FD OCT and MP-1.

Conclusions: Photoreceptor disruption after macula-off RD repair is a common abnormality in the macula that is detected better with FD OCT than Stratus OCT. A good correlation between MP-1 abnormality and presence of photoreceptor disruption or subretinal fluid on FD OCT demonstrates that these anatomic abnormalities contribute to decreased visual function after successful repair.

Financial Disclosure(s): The authors have no proprietary or commercial interest in any materials discussed in this article. *Ophthalmology* 2008;115:1923–1929 © 2008 by the American Academy of Ophthalmology.



Successful reattachment of the macula after RD is often associated with incomplete visual recovery. Preoperative factors influencing macula recovery include preoperative visual acuity, duration and height of detachment, and vitreomacular traction.¹ Postoperative clinical findings include cystoid macular edema, epiretinal membranes, retinal folds, retinal pigment epithelium (RPE) migration, and persistent subretinal fluid (SRF).¹ Even with a normal-appearing macula on examination, patients often experience visual impairment.

Optical coherence tomography (OCT) is a noninvasive imaging modality that effectively images the layers of the retina at near-histologic resolution.² To help explain visual loss after macula-off RD repair, the commercially available Stratus OCT (Carl Zeiss Meditec, Inc, Dublin, Calif) has elucidated several postoperative factors correlating with

poor vision. These features include persistent SRF and increased foveal thickness.^{3–7} Two recent studies using Stratus OCT and ultrahigh-resolution, time-domain OCT have detected disruptions in the photoreceptor layer among many subjects after RD repair.^{8,9}

Fourier-domain (FD) OCT is a novel imaging system capable of capturing images 40 to 50 times faster than the standard time-domain OCT.^{10–14} This allows real-time, in vivo, high-resolution imaging with decreased motion artifact. A rapid serial sweep of approximately 100 B-scans can render a 3-dimensional volume of the entire macula, from which *en face* C-scans can be derived. This permits localization of macular lesions that may otherwise be missed by limited radial line scans of conventional time-domain OCT.¹⁵

The FD OCT instrument constructed at our institution produces high-resolution images (4.5 μm axial, 10–15 μm calculated transverse resolution) at a high acquisition speed (10,000 A-scans/frame, 12 frames/second). Our group recently demonstrated the increased diagnostic utility of high-resolution FD OCT in imaging choroidal neovascularization, retinal angiomatous proliferation, and macular holes.^{13,14}

Fundus-related microperimetry (MP) is a functional measure of macular sensitivity. The MP-1 Microperimeter (Nidek Technologies, Padova, Italy) measures several points in the patient's central field and effectively maps out microscotomas. An infrared camera establishes and tracks the patient's fixation, and the resulting visual field is registered onto the corresponding fundus photograph. In this manner, the functional defect can be localized to the anatomic macular abnormality. Studies have shown that the MP-1 results are reproducible and comparable to standard automated perimetry.^{16,17}

The present study used the FD OCT instrument constructed at the University of California Davis Medical Center to create high-resolution B- and C-scans of the macula after anatomically successful macula-off RD repair. Correlation between morphologic changes on transverse C-scans and functional deficits as measured by MP was also determined in a subset of patients.

Materials and Methods

A chart review was performed for patients who had undergone anatomically successful reattachment surgery between January of 2005 and December of 2006 at the University of California Davis for primary, macula-off rhegmatogenous RD. Patients who had successful repair with ≤ 2 procedures or surgeries were included in this study if surgery had been performed at least 3 months earlier. Exclusionary criteria included dense media, preexisting macular conditions (e.g., age-related macular degeneration), and clinically evident postoperative changes (e.g., cystoid macular edema and significant epiretinal membrane) that were likely to affect visual outcome. Before imaging, written informed consent was obtained. The study was conducted according to a protocol approved by the Office of Human Research Protection at the University of California-Davis School of Medicine.

Demographic data collected included age, sex, ocular history, duration of preoperative symptoms, extent of RD, and surgical details. Best-corrected visual acuity (BCVA) by Snellen chart, anterior segment examination, and dilated fundus examination with indirect and slit-lamp biomicroscopy were performed on all patients. The Snellen equivalent of "counting fingers" was 20/1430.¹⁸ The 6 \times 6-mm radial line scan protocol was performed on each patient using Stratus OCT.

Each patient underwent scanning by the high-speed, high-resolution FD OCT device constructed at the University of California Davis. The images presented here were acquired using a broad bandwidth, superluminescent diode light source, model D855 (855 nm at 75 mm bandwidth, Superlum Diodes Ltd, Moscow, Russia). Axial resolution is 4.5 μm , and calculated transverse resolution is 10 to 15 μm . A set of 100 B-scans (1000 A-scans/frame, 12 frames/second), covering a 6 \times 6 \times 2-mm volume of macula (lateral \times lateral \times depth), was acquired for each patient in 8 seconds. Each B-scan was laterally separated by 60 μm . Fine axial distortion between B-scans was corrected using a correlation-

based algorithm. The registered volume (1000 \times 500 \times 100 pixels) was used as a reference for a cross-sectional extraction algorithm, which allows for construction of any B- or C-scan from the acquired data.

To improve C-scan slicing and more effectively visualize the extent of SRF, the FD-OCT images of 2 patients with high myopia were flattened with respect to the RPE to minimize the effect of the globe curvature on the C-scan. This was done automatically by finding the RPE location on each A-scan and then shifting all A-scans axially to position the RPE on the same reference C-scan.

Eleven patients also underwent functional vision testing by the MP-1 Microperimeter (Nidek Technologies). Six patients were unable to perform the test because of scheduling conflicts and limited machine availability within the department. The central 20 degrees was tested in patients with undilated pupils using a Goldmann size-III stimulus and 4-2-1 staircase. Fixation was tracked by the infrared camera, and the visual field was projected onto the corresponding fundus photograph. The test was considered reliable if $>80\%$ and $>90\%$ of fixation points were within 2 and 4 degrees of center, respectively.

To superimpose the C-scan and MP-1 images, C-scan retinal landmarks (e.g., retinal vascular patterns) were manually selected by the examiner and marked in color using Photoshop CS software (Adobe Systems Inc, San Jose, CA). The image was made transparent such that the colored marks and some anatomic features were still visible. The C-scan was then superimposed onto the MP-1 such that the marked landmarks aligned with the landmarks clearly visible on the MP-1 fundus photograph. The color marks were then subtracted from the C-scan image.¹⁹

Results

Seventeen eyes from 17 subjects were studied. Table 1 summarizes the demographic data of these 17 eyes. Mean preoperative Snellen BCVA was 20/920 (range, 20/150 to counting fingers). Thirteen patients achieved successful reattachment after 1 surgery (5 pa-

Table 1. Demographic Data of 17 Subjects Who Had Macula-off Retinal Detachment Repair

No. of patients	17
Age (y)	Mean, 56; range, 23–78
Gender	Male, 12
Estimated duration symptoms (d)	Median, 7; range, 1–1080
Preoperative BCVA	Mean 20/920; range, 20/150–1430 (CF)
Extent detachment (clock hours)	Mean, 7; range, 4–12
Lens status (No. patients)	
Phakic	10
Pseudophakic	6
Aphakic	1
PnR	9
4 Failed PnRs	2 repeat PnR 2 PPV/SB
SB	2
PPV	1
PPV/SB	5
Postoperative time until OCT (mo)	Mean, 7; range, 2–30
Postoperative BCVA	Mean, 20/78; range, 20/15–20/200
No. tested with MP1	11
No. with reliable MP1	7

BCVA = best-corrected Snellen visual acuity; CF = counting fingers; MP1 = microperimetry-1; OCT = optical coherence tomography; PPV = pars plana vitrectomy; PnR = pneumatic retinopexy; SB = scleral buckle.

tients with pneumatic retinopathy, 2 patients with scleral buckling, 1 patient with vitrectomy, and 5 patients with vitrectomy and scleral buckle). Four patients with failed pneumatic retinopathy underwent successful reattachment surgery with repeat pneumatic retinopathy (2 patients) or vitrectomy combined with scleral buckle (2 patients). Mean postoperative BCVA was 20/78 (range, 20/15–20/200).

Table 2 (available at <http://aaojournal.org>) shows the preoperative and postoperative clinical, Stratus OCT, and FD OCT findings of the subjects at least 3 months after successful reattachment surgery. Although Stratus OCT detected photoreceptor abnormalities in 2 patients (12%), FD OCT showed disruptions in the inner segment-outer segment (IS-OS) junction, or photoreceptor layer, in 13 patients (76%) ($\chi^2 = 11.930$ with Yate's correction for continuity, $df = 1$, $P < 0.001$). Persistent SRF not seen on clinical examination was detected by Stratus and FD OCT in 2 patients (12%). A lamellar hole was seen on clinical examination and OCT in 1 patient (6%). Among 9 patients (53%) who had no abnormality on clinical examination, 8 (47%) had a normal Stratus OCT and 3 (18%) had a normal FD OCT.

Figure 1 shows the retinal layers in a normal subject as imaged with the FD OCT system used in this study. The IS-OS junction of the photoreceptor layer can be clearly visualized using this system. Figure 2 demonstrates an example of a patient with photoreceptor disruptions seen more clearly on FD OCT than Stratus OCT. The *en face* C-scans illustrate the diffuse extent of these disruptions throughout the macula and localize them to the IS-OS junction.

Six of the 17 study patients did not undergo MP-1 testing because of scheduling reasons. Among the 11 patients tested with MP-1, 7 produced reliable results, that is, $>80\%$ fixation points were within 2 degrees and $>90\%$ were within 4 degrees of center. As shown in Table 3, the MP-1 results correlated with FD OCT findings in 6 of 7 patients (86%). One of these patients (Patient 7) with 20/20 vision had a normal FD OCT and MP-1. Areas of decreased sensitivity on MP-1 corresponded to areas of photoreceptor layer disruption in 4 patients, to areas of persistent SRF in 2 patients, and possibly to a lamellar hole in 1 patient (Table 3).

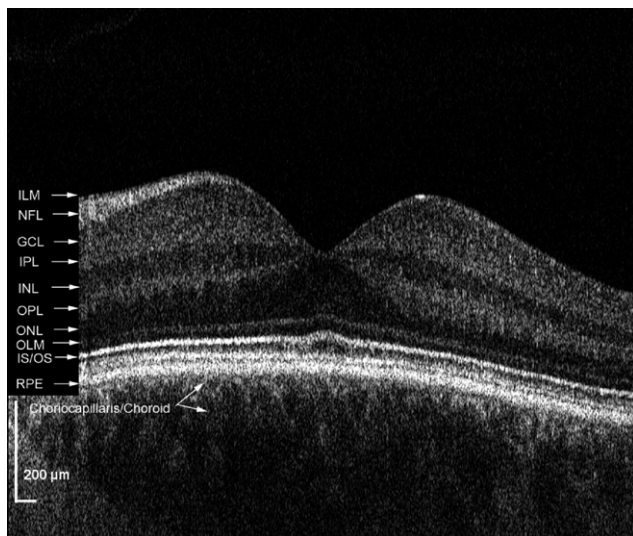


Figure 1. High-resolution FD OCT of a normal subject with retinal layers labeled. GCL = ganglion cell layer; ILM = internal limiting membrane; INL = inner nuclear layer; IPL = inner plexiform layer; IS/OS = inner segment/outer segment junction; NFL = nerve fiber layer; OLM = outer limiting membrane; ONL = outer nuclear layer; OPL = outer plexiform layer; RPE = retinal pigment epithelium.

Among the 4 patients who did not perform reliably on the MP-1, the VA was poorer and more diffuse photoreceptor disruption was noted on FD OCT in 3 patients. One patient had head tremor from Parkinson's disease and could not maintain fixation for MP-1.

Visual acuity did not always correlate with findings on FD OCT. Figure 3 shows the OCT images from an asymptomatic subject with visual acuity of 20/20 (Patient 2). Both Stratus and FD OCT B-scans showed persistent SRF extending subfoveally and temporally. MP-1 shows some loss of sensitivity in the temporal peripheral macula, in the area of more extensive SRF. The photoreceptor layer appears relatively intact within the area of SRF and in the attached portions imaged with FD OCT, perhaps resulting in lack of visual symptoms. Similarly, Patient 1 (not shown) had mild metamorphopsia and visual acuity of 20/25. FD OCT showed slight photoreceptor disruption at the fovea; MP-1 was normal (Table 3). Patient 4 (Fig 4) had visual acuity of 20/25 with central metamorphopsia. FD OCT showed a small lamellar hole and photoreceptor layer disruptions underlying the lamellar hole at the fovea with some extension superonasally.

In one subject, photoreceptor disruption and SRF were both noted on FD OCT. Figure 5 (available at <http://aaojournal.org>) shows OCT images from Patient 3 who had 20/60 vision 3 months after scleral buckle surgery. FD OCT B-scans and flattened C-scans revealed photoreceptor disruptions at and around the fovea, as well as a large area of persistent SRF nasally and small pockets inferiorly. MP-1 demonstrated diffuse decrease in sensitivity that was most pronounced nasally, in the area of persistent SRF. These findings suggest that both photoreceptor disruptions and persistent SRF may be contributing to decreased visual function in this patient.

Discussion

Incomplete macular recovery after anatomically successful RD repair has been attributed to several preoperative and postoperative factors. Previous studies have used histologic methods and time-domain OCT to describe the microstructural changes that occur in the macula after RD repair.^{8,9,19} In this report, high-speed, high-resolution FD OCT was used to visualize the retinal architecture in fine detail after macula-off RD repair. With image acquisition speeds 20 to 40 times faster than time-domain OCT, accurate 3-dimensional volumes and *en face* C-scans could be constructed to visualize the extent of these morphologic changes in the macula.

In this report, FD OCT detected subclinical disruptions in the IS-OS junction of the photoreceptor layer in 76% of the 17 study subjects. These changes were not as clearly seen on standard Stratus OCT. This is similar to a recent report that used ultrahigh-resolution, time-domain OCT to detect photoreceptor layer distortions in eyes after RD repair.⁹ A second report used Stratus OCT to detect broken or absent photoreceptor layer line in 41% of patients after macula-off RD repair, the presence of which predicted poor postoperative BCVA.⁸

Whether a decrease in reflectivity of the IS-OS junction on OCT represents absent or misaligned photoreceptors remains unknown. Histopathologic animal retina studies have shown that photoreceptors are the first structures to degenerate after detachment (at day 1), and atrophy persists after reattachment.^{19,20} Apoptosis has been shown to play a role in photoreceptor death after RD in both animals and

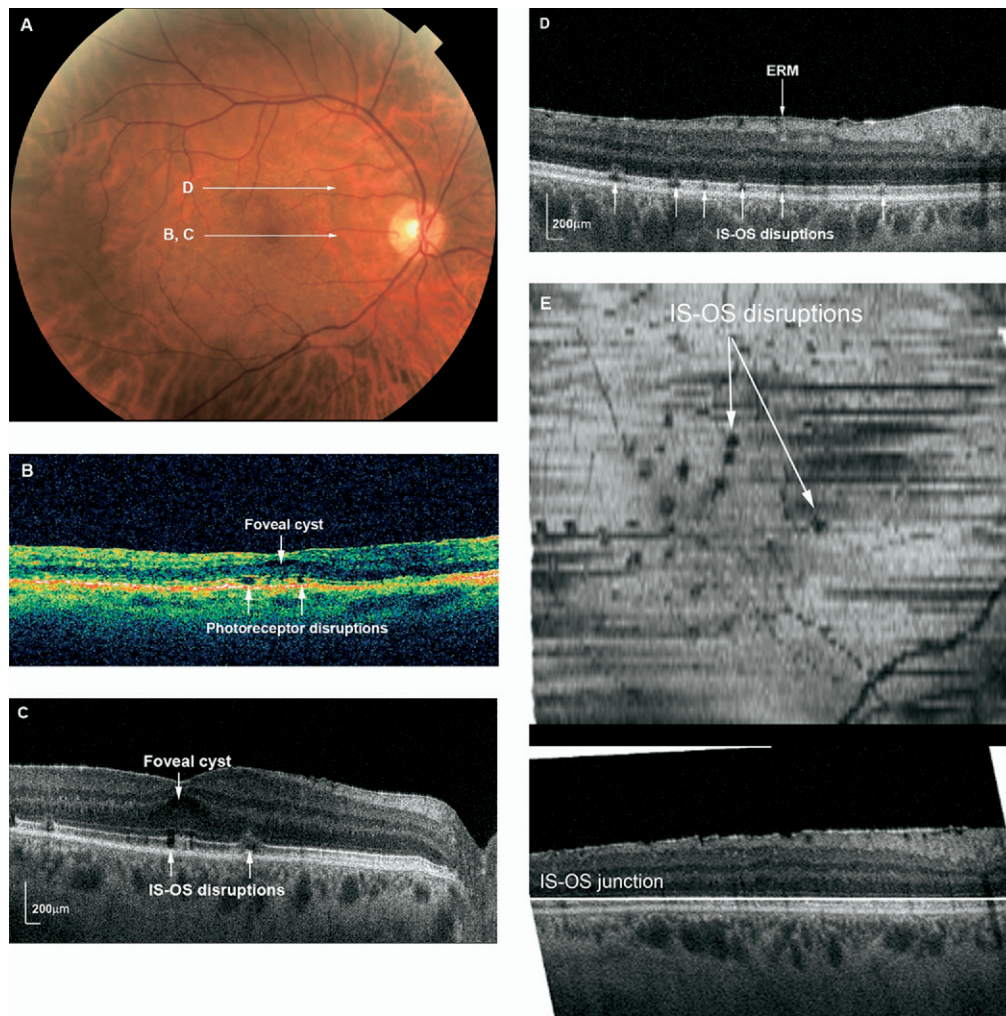


Figure 2. A, Fundus photograph of the right eye of Patient 8 shows a mild epiretinal membrane 7 months after RD repair. Visual acuity was 20/50. White arrows indicate direction of OCT scanning in corresponding figures (B–D). B, Stratus OCT showing small defects in the photoreceptor layer and a small foveal cyst. C, FD OCT B-scan through the fovea showing focal subfoveal and juxtafoveal disruptions in the photoreceptor IS-OS junction. D, Selected FD OCT B-scan through superior macula illustrating the focal photoreceptor layer disruptions scattered throughout the macula, as well as an epiretinal membrane. E, C-scan (en face) through the IS-OS junction showing the focal hypointensities throughout the macula. The horizontal line in the lower B-scan depicts the level at which the transverse C-scan is taken. ERM = epiretinal membrane; IS-OS = inner segment-outer segment.

humans.^{21–25} Although outer segment regeneration can occur, animal studies of reattachment have also shown that this regeneration occurs in a “patchwork” appearance of the RPE-photoreceptor interface.²⁴

Several previous studies showed improved visual function after retinal reattachment surgery. Ozgur and Esgin²⁶ used pattern visual evoked potential to demonstrate increased P100 latency values compared with control eyes but no difference in P100 amplitudes.²⁶ A multifocal electroretinography study of patients undergoing scleral buckle for macula-on or off RD revealed improved foveal amplitudes after surgery.²⁷ Full-field ERG in the patients with macula-off RD showed improved rod function after reattachment. Previous studies using Goldmann kinetic perimetry have demonstrated impaired recovery of sensitivity after retinal reattachment.^{28–30} One study revealed higher mean devia-

Table 3. Comparison between Fourier-Domain Optical Coherence Tomography C-scans and Microperimetry Results

Patient No.	Postoperative Vision	C-scan Findings	MP-1 Results
1	20/25	Mild PR disruption	Normal
2	20/20	SRF	Mild ↓ in SRF area
3	20/60	PR disruption, SRF	↓ in PR disruption and SRF areas
4	20/25	Lamellar hole, PR disruption	↓ in PR disruption area and lamellar hole
5	20/100	PR disruption, ERM, Mild CME	↓ in PR disruption area
6	20/30	PR disruption	↓ in PR disruption area
7	20/20	Normal	Normal

CME = cystoid macular edema; ERM = epiretinal membrane; FD = Fourier-domain; MP-1 = Microperimetry-1; OCT = optical coherence tomography; PR = photoreceptor; SRF = subretinal fluid.

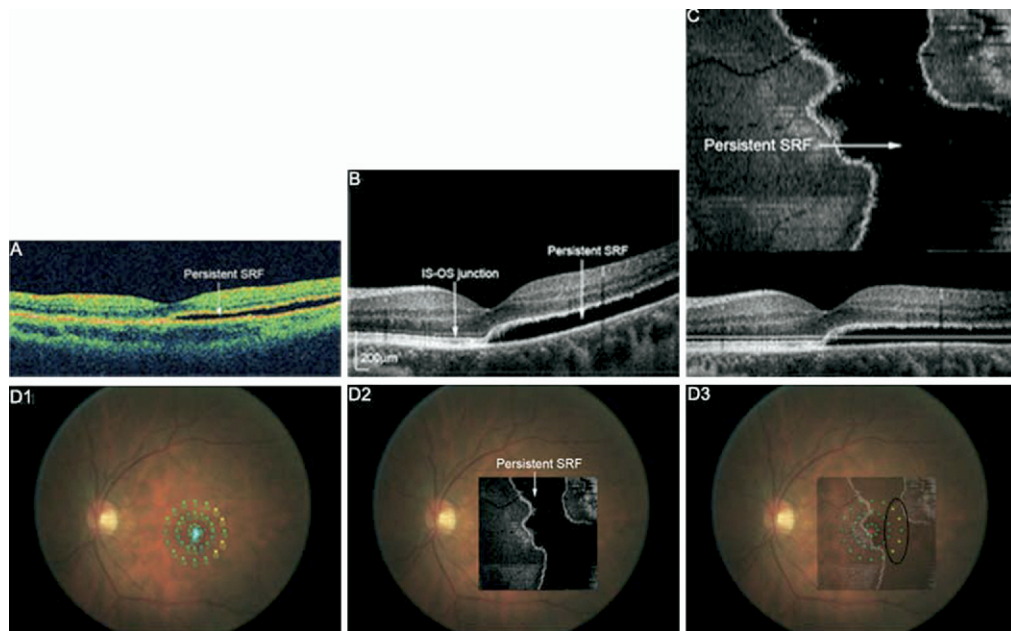


Figure 3. A, Stratus OCT of Patient 2 showing shallow SRF involving the fovea 12 months after pneumatic retinopexy. Visual acuity was 20/20, and the patient had no subjective visual symptoms. B, FD OCT B-scan also shows persistent SRF and an unremarkable photoreceptor layer (IS-OS junction) in the detached and attached macula. C, Flattened FD OCT C-scan indicating the extent of SRF in the macula. D1, MP with threshold values shown. Small, light blue dots indicate the patient's fixation. D2, Flattened C-scan overlain onto fundus photograph. D3, Flattened C-scan superimposed onto MP indicates decreased sensitivity (yellow dots) in the temporal area of persistent SRF (black circle). SRF = subretinal fluid; IS-OS = inner segment-outer segment.

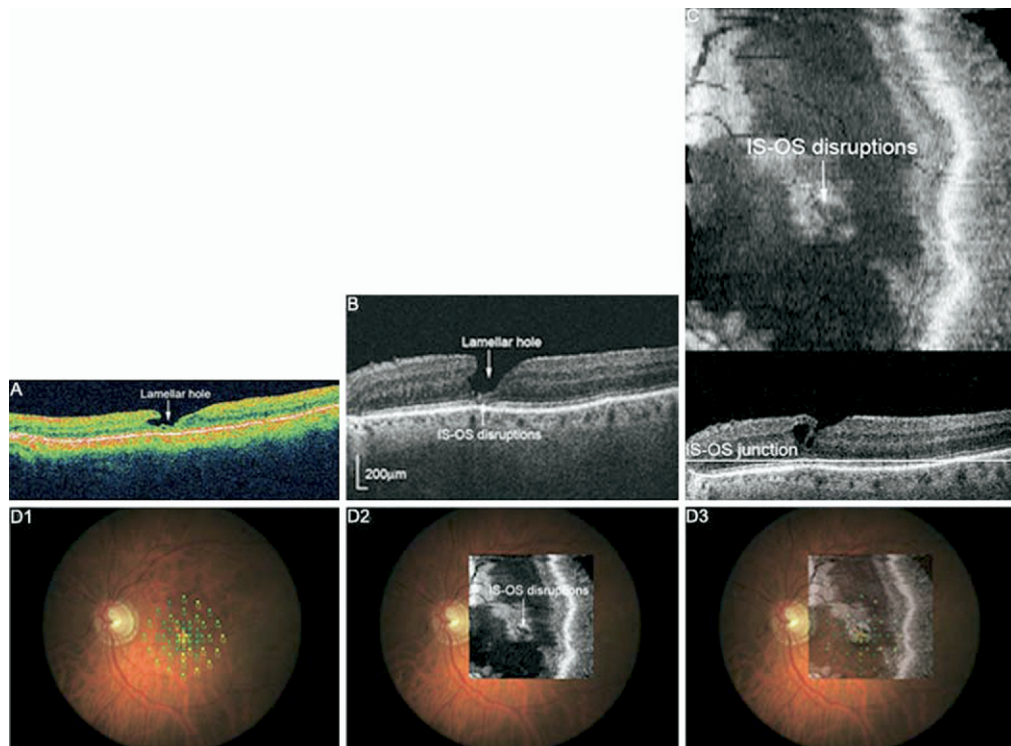


Figure 4. A, Stratus OCT of Patient 4 showing a lamellar hole at the fovea and extending nasally 30 months after vitrectomy/scleral buckle surgery. Visual acuity was 20/25, and mild metamorphopsia is noted. B, FD OCT B-scan shows the lamellar hole and subfoveal disruption of the photoreceptor layer (IS-OS junction). C, FD OCT C-scan through the photoreceptor layer shows the extent of disruption in the macula. D1, MP with threshold values. D2, C-scan overlain onto fundus photograph. D3, C-scan superimposed onto MP indicates decreased sensitivity in the area of photoreceptor layer disruption (black circle). IS-OS = inner segment-outer segment.

tions on standard automated perimetry in the reattachment eye compared with the fellow eye.²⁵

In our study, MP was used in a subset of patients to assess macular function and to correlate the abnormalities with morphologic changes seen on FD OCT. Six of 7 eyes had areas of abnormal sensitivity on MP-1. In 4 eyes, these areas mapped out to areas of disruptions in the photoreceptor layer on FD OCT C-scans. In 2 eyes, the areas of MP-1 abnormality corresponded to areas of persistent SRF. Patient 1 (Table 3) was an exception in that mild disruption at the foveal IS-OS junction was noted on FD OCT but MP-1 was normal. One possibility for this discrepancy could be that the photoreceptor changes were too minimal to be visually significant. However, given that the patient had 20/25 BCVA and noted central metamorphopsia, it is more likely that the scotoma was too small to be detected by MP-1.

Patient 4 had photoreceptor disruptions underlying a lamellar hole. The microscotoma detected on MP-1 mapped out to both FD OCT abnormalities, making it uncertain whether the decreased sensitivity was the result of photoreceptor layer disruptions, the lamellar hole, or both.

Previous OCT studies have shown that subclinical, persistent SRF occurs in a substantial number of patients after RD repair, regardless of surgical modality. Although some studies conclude that persistent SRF is correlated with poor postoperative vision,^{6,31} others found no association.³² In our study, 2 eyes had persistent SRF and both eyes had corresponding areas of decreased sensitivity on MP-1 even in the absence of visual symptoms. This is exemplified in Patient 2 (Fig 3) who had SRF involving the fovea 6 months after reattachment but had 20/20 central vision and no subjective symptoms. FD OCT showed a normal-appearing photoreceptor layer over the area of detachment. However, MP-1 revealed a mild decrease in sensitivity in the temporal peripheral macula, where there was more extensive SRF. One possible explanation for this observation is that the transport of materials between the retina and the RPE may not be affected significantly when there is mild SRF but may be increasingly affected as SRF increases.

In the case of Patient 3, both photoreceptor layer abnormalities and persistent SRF were noted on FD OCT 3 months after scleral buckle surgery. MP-1 showed a diffuse decrease in sensitivity that corresponded to the areas of photoreceptor disruptions and shallow pockets of SRF. The macular sensitivity on MP-1 was clearly worse nasally, in the area of more extensive SRF. In this case, both photoreceptor layer abnormalities and persistent SRF are likely to be contributing to the impaired visual recovery.

Limitations of this current study include the small patient number and the inability to correlate BCVA with anatomic abnormalities detected by OCT in some patients. Many patients who underwent RD repair at the University of California Davis Medical Center had complex detachments, multiple repairs, or significant postoperative changes that did not qualify them for the study. MP proved an effective way to address macular function among a subset of the study patients, but not all subjects could reliably perform

MP-1. Patients with poorer vision and more diffuse photoreceptor disruption tended to perform poorly on MP-1. Furthermore, a number of patients had concurrent macular findings, such as mild epiretinal membranes, mild cystoid macular edema detected on OCT, and lamellar hole, which may have contributed to decreased postoperative vision.

High-resolution FD OCT revealed varying degrees of photoreceptor disruption in 71% of the 17 study subjects at least 3 months after anatomically successful reattachment for macula-off RD. High-resolution FD OCT was superior to standard Stratus OCT in visualizing the photoreceptor layer and detecting these abnormalities; Stratus OCT detected these changes in only 12% of subjects ($P < 0.001$). The faster image acquisition speed of FD OCT allows construction of *en face* C-scans that could be used to visualize the extent of morphologic abnormalities throughout the macula. When superimposed onto microperimetric data, the FD OCT findings corresponded to MP-1 results in 6 of 7 patients (86%). The FD OCT abnormalities that corresponded best to decreased sensitivity on MP-1 were photoreceptor layer disruptions and persistent SRF. A future larger study using the current technology will be useful to validate our findings and to further our understanding of morphologic and functional changes associated with RD and subsequent repair.

References

1. Abouzeid H, Wolfensberger TJ. Macular recovery after retinal detachment. *Acta Ophthalmol Scand* 2006;84:597–605.
2. Huang D, Swanson EA, Lin CP, et al. Optical coherence tomography. *Science* 1991;254:1178–81.
3. Lecleire-Collet A, Muraine M, Menard JF, Brasseur G. Predictive visual outcome after macula-off retinal detachment surgery using optical coherence tomography. *Retina* 2005;25:44–53.
4. Wolfensberger TJ, Gonvers M. Optical coherence tomography in the evaluation of incomplete visual acuity recovery after macula-off retinal detachments. *Graefes Arch Clin Exp Ophthalmol* 2002;240:85–9.
5. Benson SE, Schlottmann PG, Bunce C, et al. Optical coherence analysis of the macula after vitrectomy surgery for retinal detachment. *Ophthalmology* 2006;113:1179–83.
6. Benson SE, Schlottman PB, Bunce C, et al. Optical coherence tomography analysis of the macula after scleral buckle surgery for retinal detachment. *Ophthalmology* 2007;114:108–12.
7. Avitabile T, Bonfiglio V, Sanfilippo M, et al. Correlation of optical coherence tomography pattern and visual recovery after vitrectomy with silicone oil for retinal detachment. *Retina* 2006;26:917–21.
8. Lecleire-Collet A, Muraine M, Menard JF, Brasseur G. Evaluation of macular changes before and after successful retinal detachment surgery using Stratus-optical coherence tomography. *Am J Ophthalmol* 2006;142:176–9.
9. Schocket LS, Witken AJ, Fujimoto JG, et al. Ultrahigh-resolution optical coherence tomography in patients with decreased visual acuity after retinal detachment repair. *Ophthalmology* 2006;113:666–72.
10. Wojtkowski M, Bajraszewski T, Gorczynska I, et al. Ophthalmic imaging by spectral optical coherence tomography. *Am J Ophthalmol* 2004;138:412–9.

11. Leitgeb R, Drexler W, Unterhuber A, et al. Ultrahigh resolution Fourier domain optical coherence tomography. *Opt Express* 2004;12:2156–65.
12. Cense B, Nassif N, Chen T, et al. Ultrahigh-resolution high-speed retinal imaging using spectral-domain optical coherence tomography. *Opt Express* 2004;12:2435–47.
13. Alam S, Zawadzki RJ, Choi S, et al. Clinical application of rapid serial Fourier-domain optical coherence tomography for macular imaging. *Ophthalmology* 2006;113:1425–31.
14. Truong SN, Alam S, Zawadzki RJ, et al. High resolution Fourier-domain optical coherence tomography of retinal angiomatic proliferation. *Retina* 2007;27:915–25.
15. Ko TH, Fujimoto JG, Schuman JS, et al. Comparison of ultrahigh- and standard-resolution optical coherence tomography for imaging macular pathology. *Ophthalmology* 2005;112:1922–35.
16. Springer C, Bultmann S, Volcker HE, Rohrschneider K. Fundus perimetry with the Micro Perimeter 1 in normal individuals: comparison with conventional threshold perimetry. *Ophthalmology* 2005;112:848–54.
17. Midenia E, Radin PP, Convento E, Cavarzeran F. Macular automatic fundus perimetry threshold versus standard perimetry threshold. *Eur J Ophthalmol* 2007;17:63–8.
18. Schulze-Bonsel K, Feltgen N, Burau H, et al. Visual acuities “hand motion” and “counting fingers” can be quantified with the Freiburg visual acuity test. *Invest Ophthalmol Vis Sci* 2006;47:1236–40.
19. Stopa M, Bower BA, Davies E, et al. Correlation of pathologic features in spectral domain optical coherence tomography with conventional retinal studies. *Retina* 2008;28:298–308.
20. Machemer R. Experimental retinal detachment in the owl monkey. IV. The reattached retina. *Am J Ophthalmol* 1968;66:1075–91.
21. Anderson DH, Guerin CJ, Erickson PA, et al. Morphological recovery in the reattached retina. *Invest Ophthalmol Vis Sci* 1986;27:168–83.
22. Chang CJ, Lai WW, Edward DP, Tso MO. Apoptotic photoreceptor cell death after traumatic retinal detachment in humans. *Arch Ophthalmol* 1995;113:880–6.
23. Berglin L, Algvere PV, Seregard S. Photoreceptor decay over time and apoptosis in experimental retinal detachment. *Graefes Arch Clin Exp Ophthalmol* 1997;235:306–12.
24. Arroyo JG, Yang L, Bula D, Chen DF. Photoreceptor apoptosis in human retinal detachment. *Am J Ophthalmol* 2005;139:605–10.
25. Kubay OV, Charteris DG, Newland HS, Raymond GI. Retinal detachment neuropathology and potential strategies for neuroprotection. *Surv Ophthalmol* 2005;50:463–75.
26. Ozgur S, Esgin H. Macular function of successfully repaired macula-off retinal detachments. *Retina* 2007;27:358–64.
27. Schatz P, Holm K, Andreasson S. Retinal function after scleral buckling for recent onset rhegmatogenous retinal detachment: assessment with electroretinography and optical coherence tomography. *Retina* 2007;27:30–6.
28. Chisholm IA, McClure E, Foulds WS. Functional recovery of the retina after retinal detachment. *Trans Ophthalmol Soc U K* 1975;95:167–72.
29. Zygulska-Mach H, Starzycka M, Ciechanowska A. Retinal function after surgical treatment of detachment. *Ophthalmologica* 1979;178:210–4.
30. Amemiya T, Iida Y, Yoshida H. Subjective and objective ocular disturbances in reattached retina after surgery for retinal detachment, with special reference to visual acuity and metamorphopsia. *Ophthalmologica* 1983;186:25–30.
31. Wolfensberger TJ. Foveal reattachment after macula-off retinal detachment occurs faster after vitrectomy than after buckle surgery. *Ophthalmology* 2004;111:1340–3.
32. Baba T, Hirose A, Moriyama M, Mochizuki M. Tomographic image and visual recovery of acute macula-off rhegmatogenous retinal detachment. *Graefes Arch Clin Exp Ophthalmol* 2004;242:576–81.

Footnotes and Financial Disclosures

Originally received: November 27, 2007.

Final revision: April 20, 2008.

Accepted: May 23, 2008.

Available online: July 31, 2008.

Manuscript no. 2007-1532.

Department of Ophthalmology and Vision Science, University of California Davis Medical Center, Sacramento, California.

Presented in part as a poster at the Association for Research in Vision and Ophthalmology Annual Meeting, Ft Lauderdale, Florida, May 3, 2006, and at the American Academy of Ophthalmology Annual Meeting, Las Vegas, Nevada, November 12, 2006.

Financial Disclosure(s):

The authors have no proprietary or commercial interest in any materials discussed in this article.

Supported in part by the National Eye Institute, Bethesda, Maryland (grant no. 014743 [JSW]), and Research to Prevent Blindness, New York (Jules and Doris Stein Professorship [JSW] and unrestricted departmental grant).

Correspondence:

Susanna S. Park, MD, PhD, Department of Ophthalmology and Vision Science, University of California Davis Medical Center, 4860 Y Street, Suite 2400, Sacramento, CA 95817. E-mail: susanna.park@ucdmc.ucdavis.edu.

Table 2. Clinical, Stratus, and Fourier-domain Optical Coherence Tomography Findings of 17 Eyes after Macula-off Retinal Detachment Repair

Patient No., Procedure	Preoperative BCVA	Postoperative BCVA	Clinical Findings	Stratus OCT Findings	FD OCT Findings
1, PPV/SB	CF	20/25	Trace RPE changes	Normal	Mild PR disruption
2, PnR	20/150	20/20	Normal	SRF	SRF
3, SB	CF	20/60	Normal	SRF	SRF, PR disruption
4, PPV/SB	20/150	20/25	Lamellar hole	Lamellar hole	Lamellar hole, PR disruption
5, PPV/SB	CF	20/100	Mild ERM	ERM, CME	ERM, CME, PR disruption
6, PnR×2	20/150	20/30	Normal	Normal	PR disruption
7, PnR×2	HM	20/20	Normal	Normal	Normal
8, PnR	20/400	20/50	Mild ERM	CME, PR disruption	ERM, CME, PR disruption
9, PPV/SB	CF	20/80	Mild ERM	CME	ERM, CME, PR disruption
10, PnR, PPV/SB	20/150	20/50	Normal	PR disruption	PR disruption
11, PnR	CF	20/50	Mild ERM	ERM	ERM, PR disruption
12, PPV/SB	CF	20/70	RPE changes	Normal	PR disruption
13, PnR	CF	20/40	Normal	Normal	PR disruption
14, SB	CF	20/200	RPE changes	Normal	PR disruption
15, PnR, PPV/SB	20/200	20/200	Normal	Normal	PR disruption
16, PPV	20/200	20/20	Normal	Normal	Normal
17, PnR	CF	20/15	Normal	Normal	Normal

BCVA = best-corrected visual acuity; CF = counting fingers; CME = mild cystoid macular edema; ERM = epiretinal membrane; FD OCT = Fourier-domain optical coherence tomography; OCT = optical coherence tomography; PnR = pneumatic retinopexy; PPV = pars plana vitrectomy; PR = photoreceptor; RPE = retinal pigment epithelium; SB = scleral buckle; SRF = subretinal fluid.

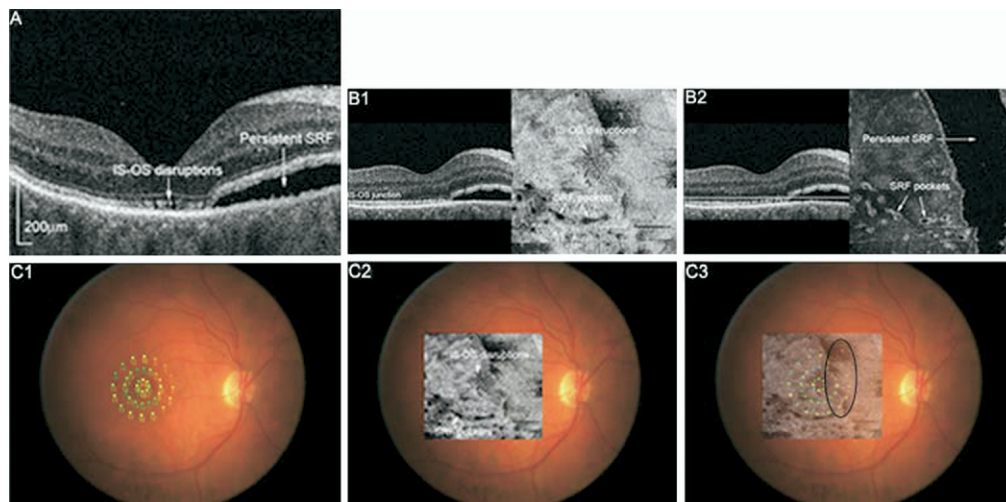


Figure 5. A, FD OCT B-scan image of Patient 3 showing photoreceptor layer disruption at the fovea and persistent SRF nasally 3 months after scleral buckle surgery. Visual acuity was 20/60. B1, Flattened C-scan through the IS-OS junction showing fine disruptions near the fovea and small pockets of SRF inferiorly. B2, Flattened C-scan slightly above the photoreceptor layer illustrates the extent of SRF in the macula. C1, MP-1 with threshold values shown. C2, Photoreceptor layer C-scan overlain onto fundus photograph. C3, Photoreceptor layer C-scan superimposed onto MP-1 indicates diffuse decrease in sensitivity diffusely and most pronounced nasally in the area of persistent SRF. IS-OS = inner segment-outer segment.